

## High- $T_c$ Superconducting Surface Coil for 2 Tesla Magnetic Resonance Imaging of Small Animals

J. Wosik, F. Wang, L.-M. Xie, M. Strikovski, M. Kamel, K. Nesteruk, M. Bilgen, and P. A. Narayana

**Abstract**—The performance of small-volume Magnetic Resonance Imaging (MRI) depends on the system noise determined by noise of a probe and/or of a preamplifier (not by the body noise). Several demonstrations confirmed that, for selected applications, high- $T_c$  superconductor MRI receiver coils have superior properties to those of comparable copper coils. We report on the outstanding performance of modified twin horseshoe YBCO rf surface probes in a 2 Tesla scanner operating at 77 K. They were used for MR imaging of spinal cord injuries in rats and for imaging of brain of small animals. The probes were designed with a virtual ground plane, thus reducing the coil-to-ground dielectric losses and making its resonant frequency less sensitive to the body proximity. Each coil was fabricated using large area 500 nm thick double-sided  $YBa_2Cu_3O_x$  films deposited on sapphire r-cut substrates. We compare the performance of the 2 Tesla high critical temperature superconductor (HTS) probe with that made of a copper coil. Designing and cryo-packaging of HTS MRI probes is discussed.

### I. INTRODUCTION

One of the recent positive news regarding applications of HTS is clear demonstration of the superiority of HTS receiver probes, in selected Magnetic Resonance Imaging (MRI) areas, over standard copper probes. MRI is a widely used diagnostic tool, which provides unsurpassed ability to image soft tissues. It is related to the phenomenon of nuclear magnetic resonance (NMR), which is based on the excitation and relaxation of nuclei (most frequently protons) within living tissues in a dc magnetic field. An excitation rf pulse at the Larmor frequency  $\nu$ , which is the precession frequency of protons in dc magnetic field ( $\nu = 21.3$  MHz for 0.5 Tesla), disturbs the equilibrium state of the nuclei. After the rf pulse, the nuclei relax to the equilibrium state with two different relaxation times ( $T_1$  and  $T_2$ ) and produce a weak decaying rf signal. In a MRI set-up, such a signal is detected by a receiver probe.

For diagnostic usefulness of this signal, its level has to be well above the noise level, thus it puts premium on signal-to-noise ratio (SNR) of the receiver probe. In addition, SNR is the fundamental restriction in achieving fast scans and high resolution required for future MRI systems.

In general, there are two regimes for conductive losses in MRI systems. The first one is sample dominated, hence the

SNR strongly depends on sample losses, while in the other one the SNR depends mainly on probe losses. In the sample (body) dominated regime, the reduction of coil ohmic losses does not give much advantage. We will discuss this case in part II of this paper. However, in the probe dominated region, when the rf receiver probe and/or preamplifier noise determines the system floor noise, SNR can be improved by decreasing the coil rf resistance. Low rf resistance of HTS materials is then very attractive.

Several demonstrations of HTS coils used for both NMR and MRI have been done up to date. It started with the work of Black and co-workers from GE on HTS probe coils for high resolution MRI microscopy at 300 MHz [1,2], was followed by the development of low-field MRI (5-20 MHz) by Conductus NMR spectroscopy coils [3,4]. In recent years, several other impressive demonstrations of HTS probes used to improve SNR were reported [5,6,7,8,9]. However, much work remains to be done in replacing the presently used copper coils by superconducting probes for selected applications. This paper shows our HTS coil designs, simulation, and images of small animals obtained using a very simple 77 K plastic cryostat with a matching and tuning circuit.

### II. SIGNAL-TO-NOISE RATIO

A probe assembly in a MRI scanner has two primary functions: a) excitation of nuclear spins in the body and b) detection of the resulting nuclear spin precession and its relaxation. During excitation, the rf coil serves as a transducer that converts the rf power into transverse rf magnetic field  $B_1$ , whereas during reception the rf coil also acts as a transducer that converts the precessing nuclear magnetization into an electrical signal.

The random noise in a MR system is caused by ohmic losses in the receiving circuit. The loss in the receiving circuit has two components: the ohmic losses in the rf coil itself and the eddy-current losses in the sample (body), which are inductively coupled to the rf coil. If we think of the coil as a series of LCR circuits, the resistance  $R$  in such a circuit is the sum of the coil resistance  $R_c$  and the resistance induced by the body conduction losses,  $R_b$ .

In MRI, the SNR is defined as the signal-to-noise voltage ratio not as the signal-to-noise power ratio commonly used in Electrical Engineering. The signal voltage, induced in the coil by a small volume of body ( $dV$ ) at a point  $\vec{r}$  can be expressed as [10]:

$$V_s = \omega_0 \left| M_T(\vec{r}) \right| \beta_1(\vec{r}) dV(\vec{r}) \quad (1)$$

where  $\omega_0$  is the resonance frequency,  $M_T(r)$  is the transverse magnetization,  $\beta_1(r)$  is coil sensitivity at  $\vec{r}$  equal to  $B_r/I$ ,

Manuscript received September 19, 2000.

This work was supported by the Texas Higher Education Coordinating Board (ARP grants 003652-238 and 092), the State of Texas via the Texas Center for Superconductivity at the University of Houston and by ISSO.

J. Wosik, F. Wang, L.-M. Xie, M. Strikovski, M. Kamel are with Texas Center for Superconductivity and Electrical and Computer Engineering Department, University of Houston

K. Nesteruk is with the Institute of Physics, Polish Academy of Sciences, Warszawa, Poland

M. Bilgen, and P. A. Narayana are with Radiology Department, University of Texas-Houston Medical School.

which is the field generated at  $\vec{r}$  by the unit current in the coil. In the volume coil,  $\beta_1$  is constant but still depends on the coil size. However, for surface coils it depends strongly on the distance from the coil.

On the other hand, using well known Nyquist equation the rms voltage noise  $V_n$  of resistance  $R$  is given by the following expression:

$$V_n = \sqrt{4k(R_c(\omega)T_{\text{coil}} + R_b(\omega)T_{\text{body}})\Delta f} \quad (2)$$

from which, with some arrangements, it yields

$$\text{SNR} = \frac{\omega_0 \int M_T(\vec{r}) dV(\vec{r}) \sqrt{N_m N_p} \sqrt{\beta_1(\vec{r})^2}}{\sqrt{4kT_{\text{body}}\Delta f} \sqrt{R_c \frac{T_{\text{coil}}}{T_{\text{body}}} + R_b(Z_p)}} \quad (3)$$

where  $k$  is the Boltzman constant,  $\Delta f$  - the bandwidth,  $T$  is the sample or body temperature,  $dV$  is the voxel volume,  $N_m$  and  $N_p$  are sample and profile numbers for image scanning, and  $Z_p$  is the distance between the coil and body.

The SNR formula can be expressed differently, in a more practical manner, where the SNR depends on the quality factor ( $Q$ ) and effective volume ( $V_{\text{eff}}$ ):

$$\text{SNR}(\vec{r}, Z_p) = A \sqrt{\frac{\beta_1(\vec{r})^2 Q(Z_p)}{\omega_0 L}} = A \sqrt{\frac{\mu_0}{\omega_0}} \cdot \sqrt{\frac{Q(Z_p)}{V_{\text{eff}}(\vec{r})}} \quad (4)$$

Here,  $L$  is inductance of the coil, ( $Q = \omega L / R$ ,  $V_{\text{eff}} = \mu_0 L / \beta_1^2$ ). The expression before the last square root in Eq. (3), which value is set by MRI system parameters, is grouped as the constant  $A$ . In this form all effects relating to the receiving coils are contained in the last factor:  $\sqrt{Q/V_{\text{eff}}}$ .

Quality factor,  $Q$ , of the coil is useful in estimating the body and coil contributions to the noise figure. It is assumed that when the ratio of the unloaded  $Q_0$  (without body losses), to the loaded  $Q$ , is larger than 3, the MRI system works in the body dominated regime.

For volume-coils,  $V_{\text{eff}}$  is a constant parameter because rf magnetic field is relatively uniform over the whole field of view. In the case of surface-coils, which include superconducting coils,  $V_{\text{eff}}$  is not constant but depends on the voxel to coil distance. Since  $V_{\text{eff}}$  is inversely proportional to the square of the coil sensitivity  $\beta_1$ , it represents the volume in which the whole rf magnetic energy is stored. It implies that smaller  $V_{\text{eff}}$  indicates higher density of the rf fields energy, therefore it produces larger signal voltage.

In a body (represented by resistance  $R_b$ ), the eddy-currents losses induced by rf magnetic field can not be avoided. However, some minimization of such losses is possible by properly optimized designs where the coils provide as high as possible an rf field  $B_1$  in the region of interest and when the coil size is matched to the size of an imaged region.

The other type of losses in the body, which we did not include in  $R_b$ , is the dielectric loss due to electric field from the coil penetrating the sample (body). It creates a capacitive coupling at the proximity to a body, which can be detected by a resonant frequency shift. The use of distributing

capacitance in the coil design, can keep the electric field away from the sample, thus minimizing the body dielectric loss. Properly designed receiver coils should be sensitive to rf magnetic fields and insensitive to rf electric fields.

Equation (3) shows that for the coil loss dominated case, the reduction of  $R_c$  may have a significant influence on SNR. Since the Nyquist's noise is a function of the product of resistance and temperature, the reduction of either one or both of these parameters will increase the SNR values. Additionally, lower temperature will also reduce preamplifier electronic noise. HTS are very attractive for such applications due to their extremely low rf losses. Epitaxial, high quality superconductors at 100 MHz have at least four orders of magnitude lower resistance than normal metals do [11].

The twin horseshoe resonator coil, presented in this work, is designed as a pair of symmetrically balanced coils with a virtual ground plane [12], [13]. In this case, the maximum voltage produced in one coil with respect to the ground is one half of what would be obtained for only one end of the coil grounded. Since there are two coils placed face to face, their voltages have opposite signs leading to voltage cancellation. In Fig. 1, the difference in electric field distribution is shown between the two-sided and single loop designs. In the case when a pair of two properly aligned loops have a dielectric (substrate) between them, the electric field is confined within the dielectric so it does not penetrate the body. Similar design principle was used for superconducting coils by Black and Whithers [2], [3].

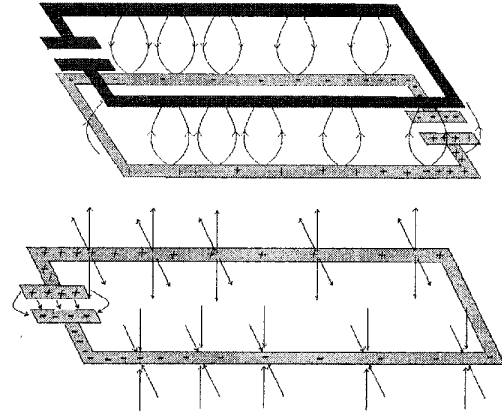


Fig. 1. Electric field lines are shown for two cases: (a) double-sided coil with distributed capacitance and (b) for a single loop design.

### III. DESIGNING OF A RECEIVER COIL

In general, a MRI coil is not a conventional rf-transmitting or receiving antenna, because the coil requires storage of magnetic energy in the near-field region. For such a resonator it is not easy to calculate inductance or capacitance from a simple quasi-static theory. To determine exact electromagnetic and geometric parameters of the design, resonating at the desired frequency, we have used the Ansoft HFSS (High Frequency Structure Simulator) package. The software is based on the finite-elements method solving a model that represents design of a high frequency device.

Fig. 2 shows the calculation model for the actual design of the twin-horseshoe receiver coil. The cylinder represents a small animal body. The diameter of the coil is 2" and the substrate is 0.5 mm thick LaAlO<sub>3</sub>. In Fig. 2a, one can see that the modeled coil resonates at the desired frequency 84.4 MHz (for the 2 Tesla scanner). The radius of the resonance Q-circle on the Smith Chart is small so it indicates small coupling through the coupling loop. The Q value obtained from these calculations for a copper twin horseshoe probe was very close to the value measured in the fabricated probe.

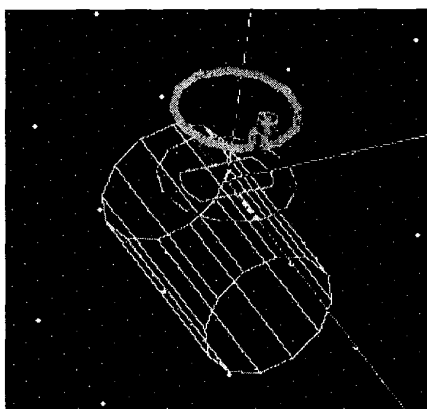
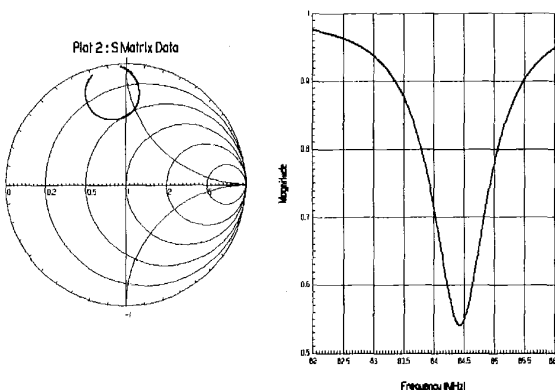


Fig. 2. Ansoft calculated resonance frequency and a coupling of twin-horseshoe coil is shown. The upper circle represents a coupling loop, the cylinder a rat body. For the simulation the coil diameter was assumed to be 2" and the LaAlO<sub>3</sub> ( $\epsilon=24$ ) substrate thickness was 0.5 mm.

Very useful for the probe design process are plots (Fig. 3) of the calculated dielectric constant ( $\epsilon$ ) dependence of on substrate thickness ( $d$ ) in the twin-horseshoe coil resonating at 84.4 MHz. The dependence of  $\epsilon$  on  $d$  is calculated for several different diameters of the same coil design, which is scaled accordingly. The dashed lines shown in Fig. 3, indicate the dielectric constants of these two substrates ( $\epsilon=9.4$ , sapphire and  $\epsilon=24$ , LAO). It can be noticed, that for commercially available sapphire substrate thickness, ranging from 0.35 mm to 1 mm, the coil diameter can be selected between 2" and 2.8."

The coils were made using patterned double-sided YBCO films deposited on 2" LaAlO<sub>3</sub> or sapphire substrates. In Fig. 4, one of our HTS probe designs is shown as an example.

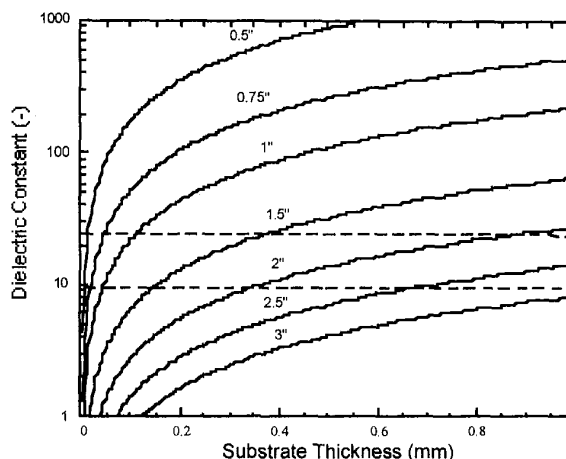


Fig. 3. Calculated relation between dielectric constant  $\epsilon$  and thickness  $d$  of a substrate used in the twin-horseshoe coil resonating at 84.4 MHz. Dependence of  $\epsilon$  on  $d$  is calculated for coil diameter ranging from 0.5 inch to 3 inches.

Measurements of the unloaded Q of an identical copper probe at room temperature and 77 K yielded  $Q = 500$  and 1000, respectively. The superconducting probe has an unloaded  $Q$ , at 77 K, of an order of 25,000.

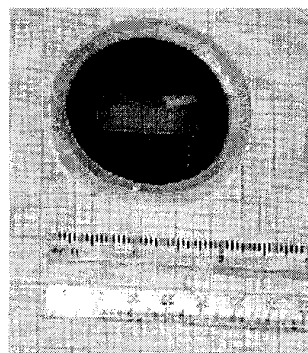


Fig. 4. A 2" in diameter twin horseshoe superconducting coil fabricated out of the double-sided 2" YBCO film on the LaAlO<sub>3</sub> substrate.

The simulated SNR dependence on distance  $Z_p$  of a coil to the voxel placed inside a phantom is shown in Fig. 5. It presents four plots corresponding to different coil sizes. Each coil has the fixed position at 2 mm from the body. A 120 mm long cylinder of radius 50 mm represents rat's body of conductivity  $\sigma = 1$  S/m. Inserts show the SNR distribution in a slice of such a cylinder for 1" (a) and 2" (b) probes. From this figure it is evident that for the small field of view, the 1" probe gives higher SNR compared to that of the 2" coil. The results obtained from the modeling were confirmed by taking MR images of rat's brain using coils of different sizes.

#### IV. IMAGING

Recent experimental results showed that the performance of our HTS coils are superior to the copper coils' performance in small animals imaging [14]. All magnetic resonance

studies were performed in a 2-Tesla custom-built scanner [15] interfaced to an SMIS Console (Surrey, UK).

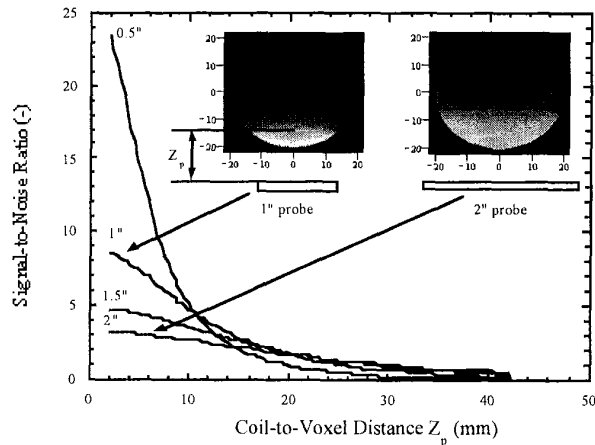


Fig. 5. Simulated SNR dependence on the distance  $Z_p$  of a coil to the voxel. The figure presents 4 plots each corresponding to a different coil size. Voxel was assumed to be inside the phantom body and a coil position is fixed at 2 mm from the body. Insets show how deep 2" (a) and 1" (b) coils see into phantom.

The cryostat with the HTS probe was inserted into a horizontal 20-cm bore superconducting magnet. The MRI protocol included the acquisition of multi-slice density-weighted (T1 or T2-weighted) images with a 0.5 mm slice thickness, a small field-of-view (FOV) of 25 mm<sup>2</sup>, and a 256 × 256 matrix size. The imaging bandwidth was 20 kHz. Prior to brain imaging, the magnetic field was always homogenized over the region-of-interest using a custom-developed auto shimming routine. The images shown in Fig. 6, represent raw data without any filtering or processing for the  $r_f$  inhomogeneity correction.

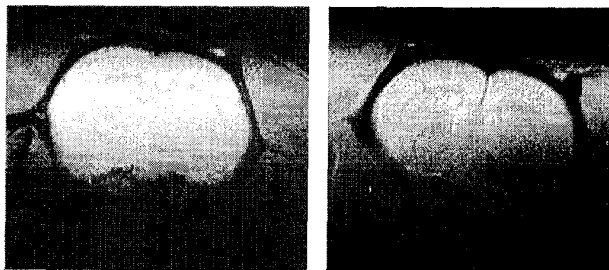


Fig. 6. Images of rat's brain acquired using a normal metal probe at room temperature (left side image) and HTS probe at 77 K (right side image).

The probe was used for both the phantom and rat imaging experiments. Images were also acquired using room temperature and 77 K copper  $r_f$  probes. Examples of axial spin echo density-weighted brain images of a rat are shown in Fig. 6. They were acquired using identical designs of copper and YBCO probes. The superconducting probe provided 2-3 times SNR gain over the normal metal probe at room temperature. The images were taken along the plane (slice) where the functional MRI experiments, using our designs, were also conducted to detect brain plasticity. Somatosensory activation from electrostimulus of forelimb or hindlimb based

on Blood Oxygenation Level Dependent (BOLD) or susceptibility contrast methodologies was used.

## V. SUMMARY

We have designed and constructed a small MRI receiver probe system for imaging small animals in a 2 Tesla small bore horizontal superconducting magnet. The system operates at 77 K and consists of a modified 2" twin-horseshoe YBCO receiver coil made out of a double sided YBCO film on LAO or sapphire substrates, a plastic cryostat, and tuning/matching mechanisms. The system needs only 10-15 minutes to be fully operational.

In imaging small animals, since the receiver probe noise dominates the performance, superconducting coils designed to minimize dielectric loss in the sample (body) gave significant SNR improvement over standard copper probes. The HTS probe design presented in this paper is superior to its copper equivalent probe providing about 2-3 times gain in SNR.

## REFERENCES

- [1] R. D. Black, P. B. Roemer, A. Mogro-Campero, L. G. Turner, and K. W. Rohling, *Appl. Phys. Lett.* (1992).
- [2] R. D. Black *et al.*, *Appl. Phys. Lett.* 62 771 (1993).
- [3] R. Black, T. Early, P. Roemer, O. Mueller, A. Mogro-Campero, L. Turner, G. Johnson, *Science* 259, 793 (1993).
- [4] R. S. Withers, G.-C. Liang, B. F. Cole, M. E. Johansson, *IEEE Trans. on Applied Superconductivity* 1, 245 (1992).
- [5] R. S. Withers, B. F. Cole, M. E. Johansson, G.-C. Liang, and G. Zaharczuk, *SPIE Proceedings Series*, Vol. 2156, High-T<sub>c</sub> Microwave Superconductors and Applications, 24-27 January 1994, Los Angeles, CA, R. B. Hammond and R. S. Withers, editors, pp. 27-35.
- [6] S.E. Hurlston, W. W. Brey, S. A. Suddarth, and G. A. Johnson, *Magn. Res. Med.* 41, 1032 (1999).
- [7] J. G. van Heteren, T. W. James, and L. C. Bourne, "Thin film HTS RF Coils for Low Field MRI," *Magnetic Resonance in Medicine*, Vol. 32, pp. 396-400, 1994.
- [8] J. R. Miller, S. E. Hurlston, Q. Y. Ma, W. Face, D. J. Kountz, J. R. MacFall, L. W. Hedlund, and G. A. Johnson, "In vivo MR Microscopy at 2T Using a Superconducting probe," *Proceedings of Magnetic Resonance in Medicine*, Vol. 1, p405, 1998
- [9] J. R. Miller, K. Zhang, Q. Y. Ma, I. K. Mun, K. J. Jung, J. Katz, D. W. Face, and D. J. Kountz, "High Sensitivity Sodium Receiver Coils for Magnetic Resonance Imaging," *IEEE Transactions on Biomedical Engineering*, Vol. 43, pp. 1997-1999, 1996.
- [10] Q. Y. Ma, "RF Applications of High Temperature Superconductors in MHz Range," *IEEE Transactions on Applied Superconductivity*, Vol. 9, No. 2, pp. 3565-3568, 1999.
- [11] M. T. Vlaardingerbroek and J. A. den Boer, *Magnetic Resonance Imaging* (Springer-Verlag Berlin Heidelberg, 1996).
- [12] Hinken, J. H., *Superconductor Electronics; Fundamentals and Microwave Application*, (Springer-Verlag, New York Berlin Heidelberg 1989).
- [13] Decorps, M., Blondet, P., Reutenauer, H., and Albrand, J. P., "An Inductively Coupled, Series-Tuned NMR Probe," *J. Magn. Resonance* 65, 100, 1985.
- [14] P. Gonord and S. Kan, "Twin-horseshoe- an investigation," *Rev. Sci. Instrum.* 65 (2), 509 (1994).
- [15] J. Wosik, K. Nesteruk, F. Wang, L.-M. Xie, M. Strikovski, M. Kamel, M. Bilgen, and P. A. Narayana, "MRI of Spine Injuries of Rats," accepted for publication in *Physica C*.
- [16] P. A. Narayana, J. L. Delayre, and L. K. Misra, *Magn. Reson. Med.* 3, 549, 1986.